EUROfusion

WPJET1-PR(17) 18026

C Marchetto et al.

Modelling the effects of an NTM island on the transport of Tungsten in JET

Preprint of Paper to be submitted for publication in
Nuclear Fusion Letter

This work has been carried out within the framework of the EUROfusion Consortium and has received funding from the Euratom research and training programme 2014-2018 under grant agreement No 633053. The views and opinions expressed herein do not necessarily reflect those of the European Commission.

Modelling the effects of an NTM island on the transport of Tungsten in JET

C. Marchetto,[1, a)] F. Koechl,[2] T. C. Hender,[3] M. Valisa,[4] M. Baruzzo,[4] T. Koskela,[5] P. Belo,[3] and JET Contributors[b)]

[1)] *Istituto di Fisica del Plasma 'P. Caldirola', via Cozzi 53, 20125 Milan, Italy*
[2)] *Technical University Wien, 1020 Vienna, Austria*
[3)] *CCFE, Culham Science Centre, Abingdon, OX14 3DB, UK*
[4)] *RFX, Corso Stati Uniti 4, Padova, Italy*
[5)] *Aalto University School of Science, Espoo, Finland*

Since 2011 the inner wall of JET has been covered with Tungsten and Beryllium tiles, replacing the previous Carbon wall (JET-C) with the ITER Like Wall (JET-ILW). In some discharges with the ILW, Tungsten accumulates in the core of the plasma, leading to a plasma radiation collapse and possibly disruption. This accumulation seems exacerbated by the presence of a magnetic island. To get an insight in this behaviour, we model a discharge with both an initially off-axis Tungsten peak and a (3,2) island. We use JETTO (a one-and-a-half-dimensional transport code calculating the evolution of plasma parameters in a time dependent axisymmetric MHD equilibrium configuration) in interpretive mode and its impurity component SANCO in predictive mode with transport coefficients set ad hoc for the off-axis W peaking. The island is modelled as an enhanced Tungsten particle diffusion zone, with radial position, time and width determined by diagnostics for that discharge. The underlying idea is that the onset of the mode suddenly changes the situation by short circuiting the region where W has accumulated, with a more central region where inward neoclassical transport dominates. The outputs of the simulations are studied in the following ways: reconstructed SXR emissivity, line integrated emissivity profiles, time evolution of SXR channels intensity, Tungsten density and radiation. A comparison between simulated and experimental data is performed for the period shortly after the island has formed.

Keywords: Transport, Tungsten, island, NTM, MHD

I. INTRODUCTION

The study of heavy impurity transport in JET dates back to the times of Carbon wall (JET-C) [see for instance[1–4]] and became of key importance with the so called Iter-Like-Wall (ILW), featuring W as the plasma-facing material in the divertor, and Be in the main chamber walls[5]. While for noble gasses such as Neon and Argon the transport appears to be anomalous[3], with medium-weight metals like Nickel and Molybdenum the transport exhibits also neoclassical characteristics[4,6]. Since the first studies, the transport of Tungsten (atomic mass 183.85) proved to be mostly neoclassical[7,8]. Experimental observations in the H-confinement mode show essentially two competing behaviours: localisation of Tungsten on the Low Field Side (LFS), due to centrifugal effects, and accumulation of Tungsten in the core, due to the peaking of the electron density[7–10].

In the literature, the transport of heavy impurities appears often influenced by the presence of Magneto HydroDynamic (MHD) activity. For Neon and Argon in hybrid scenario with JET-C the effect of an intermittent and slowly reconnecting (1, 1) mode is to worsen the W confinement, introducing two different time scales in the SXR signals evolution. The Soft X Ray (SXR) diagnostic is often used as a proxy for heavy impurity confinement because line radiation is dominated by high-Z elements[11]. The presence of a (3, 2) island does not depend on the impurity atomic number Z and completely masks the underlying occurring transport[3]. For Nickel and Molybdenum, on the contrary, the MHD modes seem to have no influence in the transport in the core and in the mid radius[3]. For Tungsten the simultaneous presence of MHD modes and impurity peaking observed in hybrid scenario JET-ILW experiments has been studied based on a database of 242 JET pulses[12]. It is experimentally observed that tearing activity with $n > 1$ can significantly enhance the rate of on-axis peaking of Tungsten impurity, while core $n = 1$ instabilities can be beneficial in removing it.

This work aims at studying the relationship between Neoclassical Tearing Modes (NTMs) and Tungsten (W) accumulation. It specifically focuses on what happens when there is an initial localisation of Tungsten on the LFS and the island appears near the same position. This subject has already been qualitatively addressed by means of two different models[12]. In the so called *indirect effect model*, the island affects the background Deuterium fuel ion profiles, which in-turn alters neo-classical and turbulent transport of the Tungsten impurity. In the *direct effect model*, which is the subject of this paper, the island changes the topology of the magnetic field lines, allowing for the parallel transport of the Tungsten to come into play. In the island region, rather than computing from first principles the transport coefficients, we add a zone of significantly enhanced diffusivity whose value is chosen through heuristic considerations (see section 3). When this model is included into a simulation of electron and main ion transport, the match between computed

[a)] marchetto@ifp.cnr.it
[b)] See the author list of "X. Litaudon et al 2017 Nucl. Fusion 57 102001"

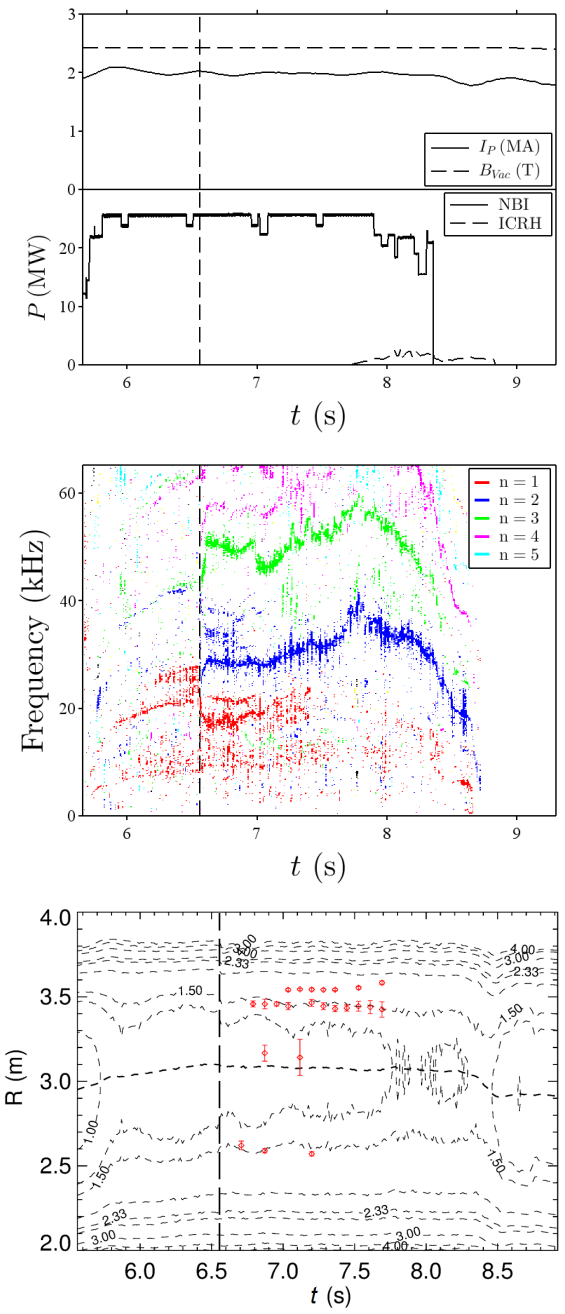

FIG. 1. Top: characterisation of JET pulse 84812. Middle: toroidal mode spectrogram given by the FFT analysis of Mirnov coils. Bottom: q contour plot (black) and island position (red dots) and size (red vertical lines) from ECE fluctuations. The vertical dashed lines represent the onset of the island at t=6.56 s.

and experimental electron density and temperature profiles improves significantly[13]. This work extends the previous studies to the case of heavy ion impurity transport. As we will see, the match with experimental data in this case holds only for the first tens of milliseconds after the island appearance.

In section 2 we describe the experimental result to be compared with the model one, and how we model the state just before the island appearance. In section 3 we describe the model for the island that has been implemented in JETTO/SANCO. In section 4 the modelling results are compared with the experimental data. In section 5 and 6 we show how the effect of the NTM in Tungsten accumulation varies with the magnitude of the enhanced island transport and with its position. We summarise and draw some conclusions on section 7.

II. EXPERIMENTAL STARTING POINT AND ITS MODELLING

As an example of a discharge with both an initial off axis Tungsten peak and a (3,2) island, we choose JET pulse 84812. This pulse was analyzed in[12] as it belongs to the data base therein described. Its main parameter are shown in Fig. 1, Top.

To study the effect of a magnetic island forming on top of a LFS Tungsten accumulation, it is first necessary to characterise the MHD activity of the discharge around this position. The MHD relevant diagnostics and techniques are described in[14], and references therein. The presence of the NTM modes is detected with Mirnov coils placed inside the torus, which probe the magnetic field perturbation produced by the mode inside the plasma. At the instant of Tungsten accumulation (see later) we see that the most intense mode is roughly at 30 kHz (the amplitude of the 50 kHz mode is an order of magnitude smaller, when measured at the wall). A Fourier transform in space allows us to determine that the mode at this frequency is n = 2 (Fig. 1, Middle). We deter-

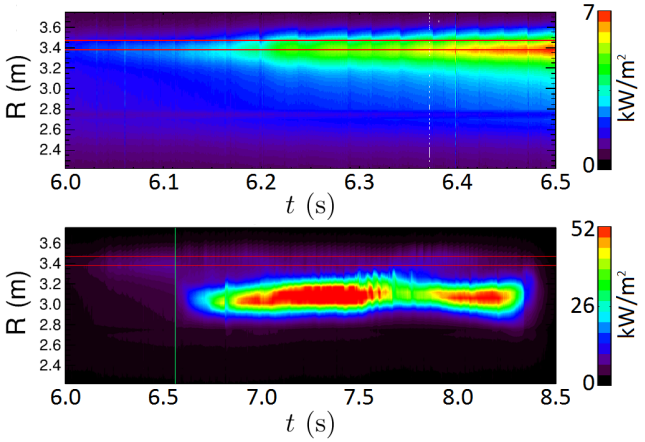

FIG. 2. Contour plot of SXR emission for JET pulse 84812. The green vertical line indicates the instant of island appearance and the red horizontal lines the island position and width, as determined in Fig. 1. The island appears at t = 6.56 s at the same position (R = 3.4 m) in which, between t = 6.00 and 6.56 s, the SXR emissivity has its relative maximum. The top figure shows a zoom into this region.

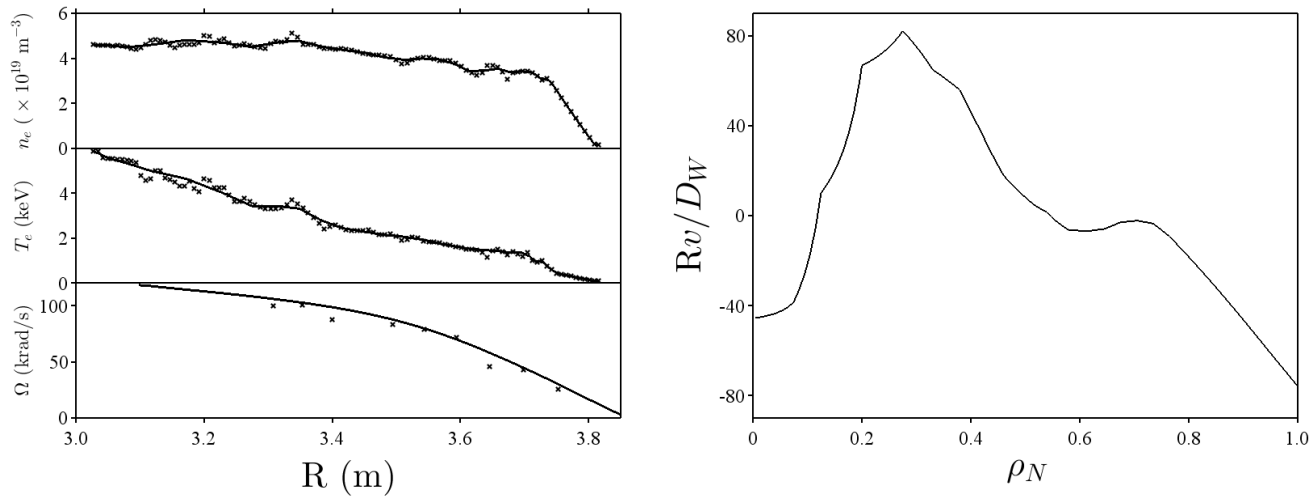

FIG. 3. Input profiles from experimental data just before the island onset, the stars mark experimental data and the solid lines are the smoothing applied by JETTO(from top to bottom: electron density and electron temperature from high resolution Thomson scattering, angular frequency from charge exchange) and transport coefficients used to simulate the pre-island state.

mine that it is a tearing and not a kink mode, i.e. that there is an island, using the electron temperature profile evolution provided by a radiometer sensitive to Electron Cyclotron Emission (ECE). Cross correlation analysis between the Mirnov signal and ECE signals shows a radial phase profile with a phase-jump whenever an island is crossed.

The coherence algorithm is used to measure the ECE fluctuation amplitude. The electron temperature gradient in the vicinity of the island is then used, together with the fluctuation amplitude, to estimate the island width. Finally, as the the mode localization obtained from ECE data follows nicely the q = 1.5 magnetic surface (Fig. 1, Bottom), we conclude that it is a (3,2) island (Tab. I).

The presence and distribution of Tungsten in the chamber can be detected analysing the SXR emission by means of cameras in different positions around the poloidal section, each of which explores an array of lines of sights. Before using this method, we compared the emissivity of the other elements contributing to Zeff in this discharge and found that Tungsten was responsible for more than 75% of the radiation. In JET pulse 84812, the SXR emission is initially peaked off-axis at R = 3.4m. After the NTM onset, the SXR emission peak moves toward the centre (Fig. 2).

To simulate the effect of the island appearing near the LFS localisation of Tungsten, we need to prepare a starting point for the simulation that has the same Tungsten distribution found in experimental data. We run JETTO (a one-and-a-half-dimensional transport code calculating the evolution of plasma parameters in a time dependent axisymmetric MHD equilibrium configuration[15]) in interpretive mode. We use input profiles (electron density and temperature and toroidal angular frequency) that are constant in time and measured immediately before the island onset (Fig. 3).

We run SANCO (the JETTO module computing impurity behaviours[16]) in predictive mode, with ad hoc transport coefficients determined to give Tungsten LFS accumulation (Fig. 3). This is a technique already exploited for instance in[8], where successful simulation of the exper-

Onset	Frequency	Position	Width	Periodicity
6.56 s	25 kHz	R = 3.4 m	10 cm	(3,2)

TABLE I. Island parameters as measured through MHD analysis.

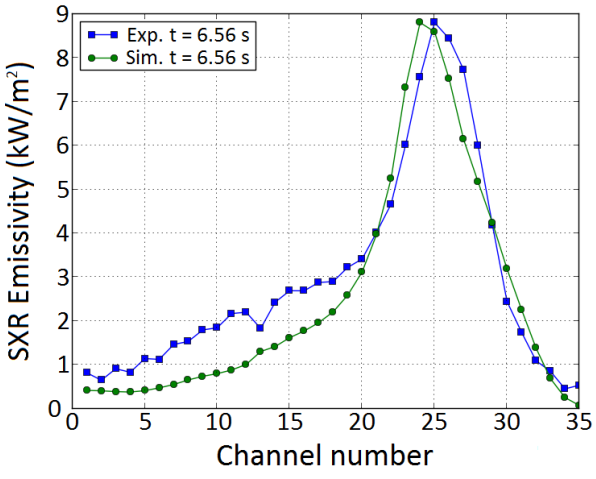

FIG. 4. Line integrated SXR emissivity calculated with SXRPY[19] for JET pulse 84812: comparison between experiment (blue) and simulation (green).

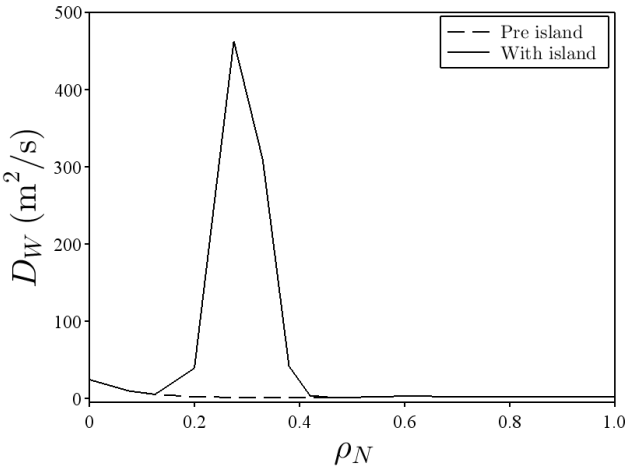

FIG. 5. Diffusivity used in SANCO to model the presence of a magnetic island as a function of normalised radius. In dashed the diffusivity without island (same as used in Fig. 3).

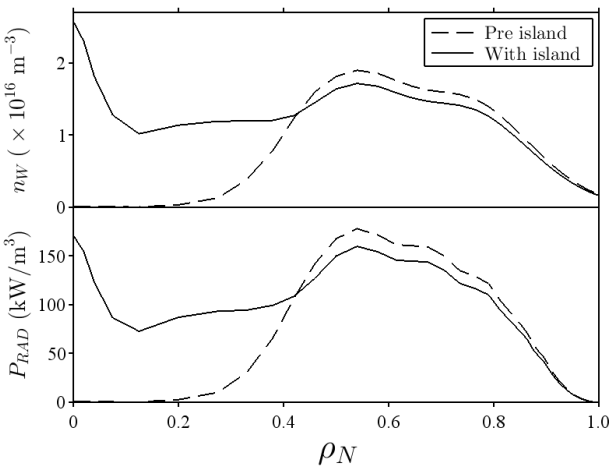

FIG. 6. Effect of the magnetic island on W density (top) and radiated power (bottom) profiles as a function of normalised radius. The quantities before the island onset are represented by dashed lines.

imental data, namely the SXR emission profile, has been achieved using as transport parameters for W those derived by NEO[17] and GKW[18] for the neoclassical and turbulent components, respectively. We calculate the simulated SXR emissivity including centrifugal effects[19] at different times and compare it with the experiment (see section 4) until a match is found (Fig. 4).

III. THE NTM MODEL IMPLEMENTED IN JETTO/SANCO

The NTM model that we implemented in JETTO/SANCO enhances the particle diffusion coefficients in the island region using a Gaussian profile. The Gaussian profile is centred on the island position, twice the sigma of the Gaussian is equal to half the island width, and the height of the Gaussian is the value of the particle diffusion coefficient inside the island (Fig. 5). Since the NTM evolves on a time scale much faster than that of transport processes, the island can be considered as saturated and its width, position and diffusion coefficient are kept constant. They form the input parameters of the model. Here, the island position and width, as we saw, are taken from the experimental data, and the diffusion coefficient is the free parameter. It is possible to model one or more islands with different positions, widths and diffusion coefficients at the same time. The model is similar to the one described in[20] and has already been tested in JETTO[13].

A random walk approach can be used to make a heuristic justification of the island transport enhancement. Taking the island width, W_{isl}, as the step the particle can do in radial direction, the diffusion coefficient is then W_{isl}^2/t where t is the time to diffuse one connection length r_c : $t = r_c^2/D_{W\|}$. The parallel diffusion coefficient of the Tungsten is given by the usual random walk argument: $D_{W\|} = v_{thW}^2/\mathbf{f}_W$ where $\mathbf{f}_W = \sqrt{2}(m_D/m_W)(Z_W/Z_D)^2\mathbf{f}_D$ and $\mathbf{f}_D$ is the Deuterium collision frequency. For a plasma of a temperature of 3 keV and a density of 6×10^{19} m^{-3}, and assuming the Tungsten in the ionised state of W^{40+}, the Tungsten perpendicular diffusion coefficient due to the island is $D_{W,island} \approx 486/q_{isl}^2$ m^2/s, where q_{isl} is the safety factor relative to the island centre. An estimate for q_{isl} from[21] shows that it can vary between O(1) and O(10) depending on details of the island ellipticity. This heuristic estimate thus gives values of $D_{W,island}$ that are consistent with those we found to affect the core tungsten evolution (see section 5).

IV. COMPARISON BETWEEN SIMULATION AND EXPERIMENTAL DATA

For the present study, as JETTO is used in interpretive mode, only the impurity transport coefficient (SANCO module) is changed by the island. Since the interplay between island and plasma is a complicated phenomenon, for this study we choose to *isolate* the effect of the island on impurity transport coefficients and to not evolve the other physical quantities.

When this model is used to simulate JET pulse 84812, which, before the island, has a localisation of Tungsten on the LFS (see section 2), there is a peaking of the Tungsten density and of the radiated power toward the centre of the plasma (Fig. 6) that grows for the first tens of milliseconds and then saturates (see sections V and VI for details). This is also seen in the contour plot of the soft X emissivity (Fig. 7) provided by the code SXRPY[19]. This software distributes in space the W-densities from

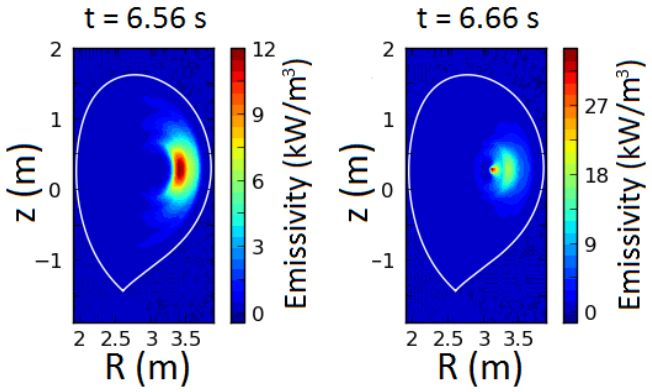

FIG. 7. Contour plot of SXR emissivity (poloidal section) calculated from the simulated W density via SXRPY. Left: initial state, before the onset of the island. Right: at island saturation.

JETTO/SANCO accounting for the centrifugal effects due to plasma toroidal rotation[22]. The emissivity is then calculated using ADAS coefficients, along the same lines of sight of the SXR diagnostic.

We compare the line-integrated emissivity calculated with SXRPY for the simulation and the experiment, before and after the appearance of the island (Fig. 8). The simulated final emissivity increases and peaks toward the centre, so the trend is similar to the experimental one but the experimental level is not reached because of the saturation. If we restrict ourselves to the first tens of milliseconds, though, the choice of not evolving the other physical quantities, above mentioned, is justified, as electrons and Deuterium are transported at a larger time scale.

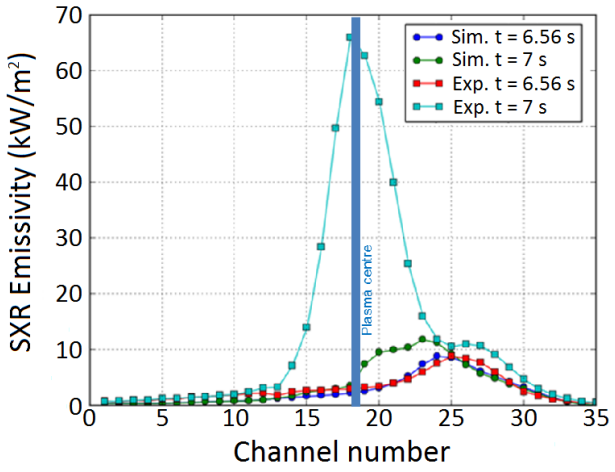

FIG. 8. Line integrated SXR emissivity before and after the island onset: comparison between experiment and simulation.

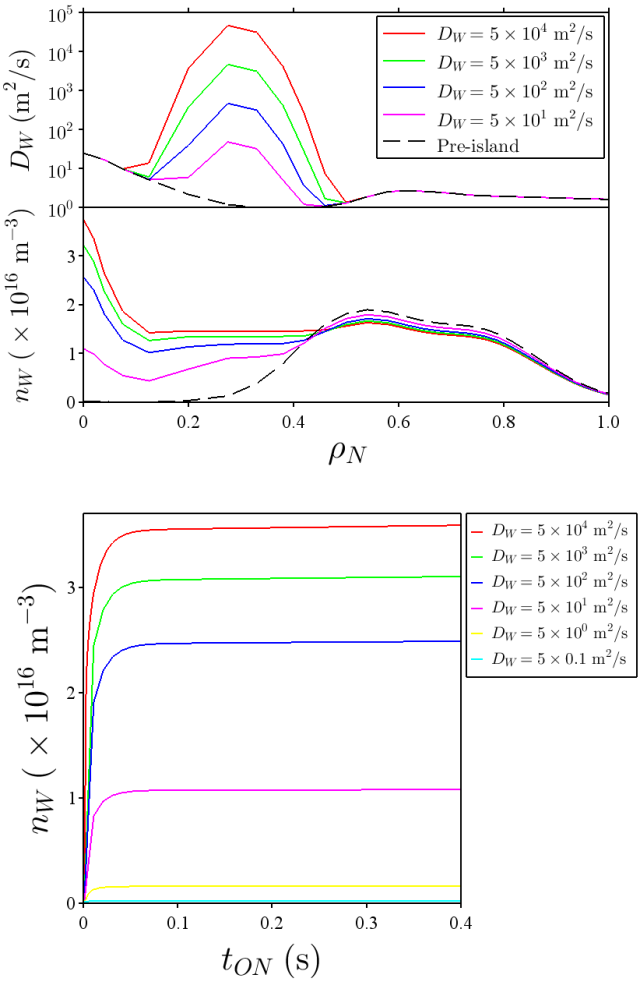

FIG. 9. Profile of W diffusivity and density (Top) and time evolution of W density at plasma centre (Bottom) for different island diffusion coefficients. In the top, the profiles without the island are given by dashed lines. The time $t_{ON} = 0$ s marks the island onset.

V. SENSITIVITY SCAN ON THE DIFFUSION COEFFICIENT VALUE INSIDE THE ISLAND

Since our model is heuristic, it is necessary to measure the effect, on the central Tungsten peaking, of different values of diffusion coefficient inside the island. Furthermore, in order to assess if the effect of the island is cumulative in time, we perform the simulations for extremely long times and examine the time evolution of the Tungsten density at the centre of the plasma (Fig. 9).

We see that the effect of the island on central W density saturates with time at different values and with different slopes for different island diffusivities. We define the *saturation time* as the time at which the central W density stops growing (i.e. when $(1/n_{W,0})(\partial n_{W,0}/\partial t) < 0.05$) and the *saturation level* as the density reached at the saturation time. One could expect that the higher the diffusion coefficient in the island, the faster the satura-

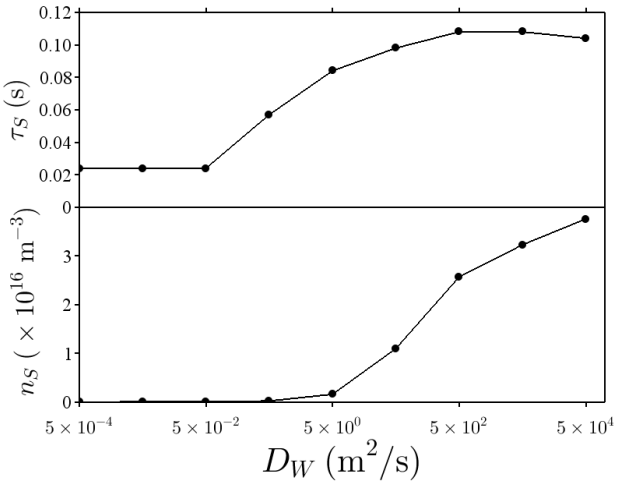

FIG. 10. Saturation time and normalised Saturation Level as function of island diffusivity.

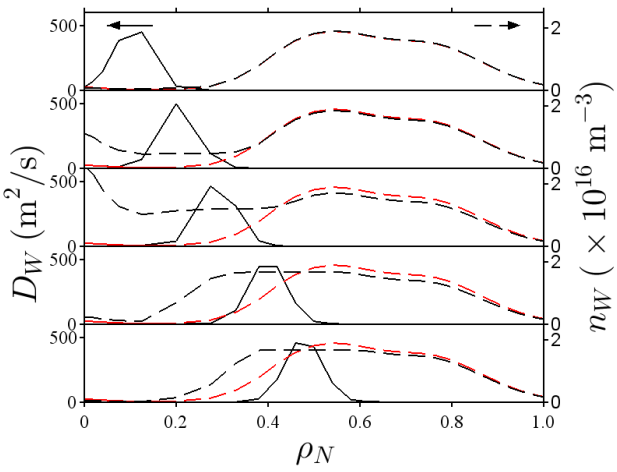

FIG. 12. Island diffusivity (solid black, left scale) and W density (dashed black, right scale) for 5 different values of the island position. In dashed red the same quantities without island. The first, third and fifth values are indicated in Fig. 13.

tion. On the contrary, the saturation time and level grow as the diffusion coefficient in the island grows (Fig. 10), suggesting we might be in presence of an additive phenomenon (it takes more time to accumulate more Tungsten). Moreover, the variation of both quantities as function of the island diffusion coefficient is negligible for low values and appears to saturate for high values (Fig. 10). This behaviour is confirmed also in the line-integrated emissivity (not shown here). The results show the island diffusivity starts to have an effect at O(10) m^2/s and is significant for O(100) m^2/s.

To compare the time evolution of the simulation results with the time evolution of the experiment, we plot the two central SXR channels (T18 and T19) from the experiment, and from the different simulations, starting from the instant of island onset (t_{ON}). The simulated emissivity is calculated by the synthetic diagnostic UTC, SANCO's postprocessor code, which generates simulated diagnostic signals using plasma profiles from transport code simulations (Fig. 11). The trend of rising SXR emission is reproduced for the first 40 ms; beyond that time other phenomena come into play.

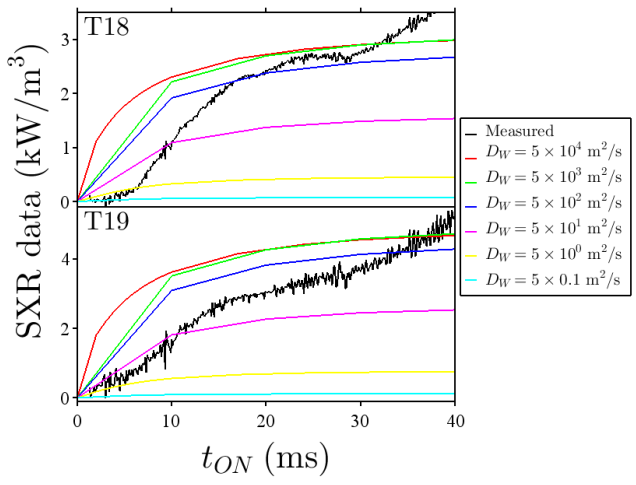

FIG. 11. SXR emissivity at the centre of plasma (channels T18 and T19): comparison between experimental data and simulation at different levels of island diffusivity.

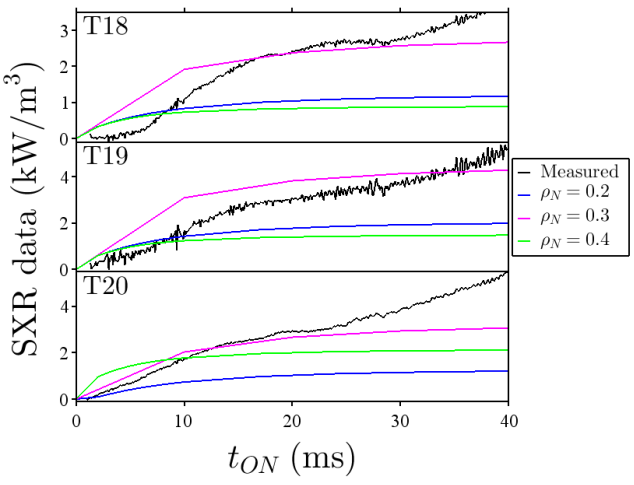

FIG. 13. SXR emissivity time evolution: comparison between experimental signal and simulated ones at different island positions, for three relevant channels.

VI. SENSITIVITY SCAN ON THE RELATIVE POSITION OF THE ISLAND AND OF THE TUNGSTEN PEAKING

For JET pulse 84812, experimentally, the island appears near the initial radial position of the Tungsten peak (Fig. 2). There is an error bar (not shown here) both on island and on Tungsten peak position measures. Moreover, it is important to assess if the effects we described in the previous sections are sensitive to the relative position of the island and the Tungsten density peaking. For these purposes, we performed a sensitivity scan with the same initial Tungsten density distribution and island diffusion coefficient, varying the radial position of the island.

The effect of the island location on peaking the emissivity in the centre is most significant for $\rho_N = 0.3$: for lower values (inner island) the emissivity tends to peak at centre but the effect is lower, while for higher values (outer island) the emissivity rises but there is no peaking at centre. If we compare the radial profile of the diffusion coefficient with the radial profile of the Tungsten density, we see that, to have an effect on W density profile, the island must be in the inner, convex part of the W density gradient (Fig. 12).

The comparison between the simulated and experimental SXR signal time evolution also shows that the simulation best reproduces experiment for an island at $\rho_N = 0.3$ (Fig. 13). Again it should be pointed out that discrepancies in the core SXR (T20) and long-time behaviour are due to phenomena not accounted for in our simulation.

VII. CONCLUSIONS

We simulate a JET-ILW discharge where both a (3,2) magnetic island and Tungsten accumulation are present, with the purpose of studying the effects of the island on W transport. We consider the SXR emissivity as a proxy for the Tungsten distribution. In order to illustrate the *direct effect* mentioned in[12], we use the 1.5 dimensional transport code JETTO in interpretive mode and its impurity module SANCO in predictive mode to simulate W transport in a NTM island. The initial experimental SXR emissivity is localised in the low field side and the island is the same radial position, causing the emissivity to evolve to be on-axis. We choose the initial state of the simulation to give the SXR emissivity comparable with experiment, situating the simulated island at the position measured in the experiment.

The final state of the experiment is a centrally peaked line integrated SXR emissivity. In the final state of the simulation, the line integrated emissivity peak has moved toward the core, saturating after the first tens of ms after the island appearance at a value lower than the experimental one. The value of the central peak for the simulated W density and the central SXR emissivity increase when the island diffusivity increases, showing a saturation for high values. This suggests that we might be in presence of an additive phenomenon. A scan on the position of the island, keeping the island diffusivity constant, shows that, to have an effect on the core Tungsten evolution, the island must be in the inner, convex part of the W density gradient. The effects on SXR emissivity confirm this. The time evolution of SXR in channels T18-T20 shows that the model reproduces the changes of slope for the first 0.04 s. This suggests that the *direct effect*of the island on W transport might be just a trigger for the influx in the first few ms. After that, other phenomena should come into play, probably linked to the evolution of the background plasma on the Deuterium transport timescale (*indirect effect*).

VIII. ACKNOWLEDGEMENTS

Useful discussions with M. Sertoli are gratefully acknowledged. Special thanks to S. Schmuck for preparing the figures.

This work has been carried out within the framework of the EUROfusion Consortium and has received funding from the Euratom research and training programme 2014-2018 under grant agreement No 633053. The views and opinions expressed herein do not necessarily reflect those of the European Commission.

One of the authors (T.C. H.) was partly funded by the RCUK Energy Programme [grant number EP/P012450/1].

[1] L.C. Ingesson et al., *Nucl. Fus.*, **38** (1998).
[2] H. Chen et al., *Phys. Plasmas*, **7** (2000).
[3] C. Giroud et al., *Nucl. Fus.*, **47** (2007).
[4] M. Valisa et al., *Nucl. Fus.*, **51** (2011)
[5] G. F. Matthews et al., *2011 Phys. Scr.*, **T145** (2011)
[6] S. P. Hirschman, D. J. Sigmar, *Nucl. Fus.*, **21** (1981)
[7] T. Puetterich et al., *Plasma Phys. Control. Fusion*, **55** (2013)
[8] C. Angioni et al., *Nucl. Fus.*, **54** (2014)
[9] F. Casson et al., *Plasma Phys. Control. Fusion*, **57** (2015)
[10] C. Angioni et al., *Phys. Plasmas*, **22** (2015)
[11] B. Alper et al., *Rev. Sci. Instrum.*, **68** (1997)
[12] T.C. Hender et al., *Nucl. Fus.*, **56** (2016)
[13] C. Marchetto et al., *Proc. of 41th EPS Conference on Plasma Physics*, Berlin, Germany, 2014.
[14] M. Baruzzo et al., *Plasma Phys. Control. Fusion*, **52** (2010)
[15] M. Romanelli et al., *Plasma Fusion Res.*, **9** (2014) and references therein
[16] L. Lauro-Taroni et al., *Proc. of 21st EPS Conference on Plasma Physics*, Montpellier, France, 1994.
[17] E. Belly, J. Candy, *Plasma Phys. Control. Fusion*, **50** (2008)
[18] A. G. Peeters et al., *Comput. Phys. Commun.*, **180** (2009)
[19] T. Koskela et al., *Plasma Phys. Control. Fusion*, **57** (2015)
[20] Z. Chang, J.D. Callen, *Nucl. Fus.*, **30** (1990)
[21] A. Biancalani et al., *Phys. Plasmas*, **17** (2010)
[22] M. Romanelli and M. Ottaviani, *Plasma Phys. Control. Fusion*, **40** (1998)